PLOS GENETICS

RESEARCH ARTICLE

The C-terminal domain of Hsp70 is responsible for paralog-specific regulation of ribonucleotide reductase

Laura E. Knighton, Nitika, Siddhi Omkar, Andrew W. Truman*

Department of Biological Sciences, The University of North Carolina at Charlotte, Charlotte, North Carolina, United States of America

* atruman1@uncc.edu

Citation: Knighton LE, Nitika , Omkar S, Truman AW (2022) The C-terminal domain of Hsp70 is responsible for paralog-specific regulation of ribonucleotide reductase. PLoS Genet 18(4): e1010079. https://doi.org/10.1371/journal.pgen.1010079

Editor: Patricija van Oosten-Hawle, University of Leeds Faculty of Biological Sciences, UNITED KINGDOM

Received: February 7, 2022

Accepted: March 21, 2022

Published: April 13, 2022

Data Availability Statement: All relevant data are within the manuscript and its Supporting Information files.

Funding: AWT was funded through the National Institutes of Health, grant numbers R01GM139885 and R15GM139059. The funders had no role in study design, data collection and analysis, decision to publish, or preparation of the manuscript.

Competing interests: The authors have declared that no competing interests exist.

Abstract

The Hsp70 family of molecular chaperones is well-conserved and expressed in all organisms. In budding yeast, cells express four highly similar cytosolic Hsp70s Ssa1, 2, 3 and 4 which arose from gene duplication. Ssa1 and 2 are constitutively expressed while Ssa3 and 4 are induced upon heat shock. Recent evidence suggests that despite their amino acid similarity, these Ssas have unique roles in the cell. Here we examine the relative importance of Ssa1-4 in the regulation of the enzyme ribonucleotide reductase (RNR). We demonstrate that cells expressing either Ssa3 or Ssa4 as their sole Ssa are compromised for their resistance to DNA damaging agents and activation of DNA damage response (DDR)-regulated transcription. In addition, we show that the steady state levels and stability of RNR small subunits Rnr2 and Rnr4 are reduced in Ssa3 or Ssa4-expressing cells, a result of decreased Ssa-RNR interaction. Interaction between the Hsp70 co-chaperone Ydj1 and RNR is correspondingly decreased in cells only expressing Ssa3 and 4. Through studies of Ssa2/4 domain swap chimeras, we determined that the C-terminal domain of Ssas are the source of this functional specificity. Taking together, our work suggests a distinct role for Ssa paralogs in regulating DNA replication mediated by C-terminus sequence variation.

Author summary

Cells require molecular chaperones to fold proteins into their active conformation. A major mystery however is why cells express so many highly-related and apparently redundant Hsp70 paralogs. We examined the role of four Hsp70 paralogs in budding yeast (Ssa1, 2, 3 and 4) on the activity of the ribonucleotide reductase (RNR complex). Importantly, we demonstrate there is selectivity of RNR subunits for Ssa1 and Ssa2 subunits, which is dictated by the co-chaperone Ydj1. Taken together, our work provides new insight into the functional specificity of Hsp70 paralogs using a native client protein.

Introduction

Cells in all organisms must be able to cope with stressors that trigger both protein unfolding and misfolding. The core machinery induced in response to challenges of proteostasis are the molecular chaperones or Heat Shock Proteins [1,2]. The essential chaperone Heat Shock Protein 70 (Hsp70) is a main player in proteostasis, binding nascent chains and responsible for stabilization, folding and degradation of a large majority of the proteome [1,3,4]. Structurally, Hsp70 chaperones comprise of three major functional domains; an N-terminal ATPase domain (NBD) connected by a flexible linker to a substrate binding domain (SBD) [2]. The SBD can be delineated further into the SBD beta "basket" into which substrates dock, the SBD beta "lid" which traps substrates for folding. The SBD is followed by an unstructured C-terminal domain (CTD) which is responsible for binding a variety of co-chaperone helper proteins [2]. The binding and hydrolysis of ATP in the NBD promotes a range of conformational changes which are transduced through the linker into the C-terminus of Hsp70 resulting in clamping of the lid over the SBD basket trapping clients and promoting protein folding [2]. Hsp70 requires the assistance of co-chaperone proteins comprised of J-proteins and nucleotide exchange factors (NEFs) that facilitate the stimulation of Hsp70 activity and folding of client proteins [3,5,6]. Although the exact mechanism by which Hsp70 folds clients remains unclear, recent evidence suggests that Hsp70 works like a molecular "hair straightener", pulling out kinks in non-optimal protein conformations, allowing correct folding to occur [7–11].

Given their role in protein folding, it is unsurprising that Hsp70 appears to exist in most organisms studied so far and is essential for their viability [2]. However, the cellular rationale for the large number of highly related paralogs of Hsp70 remains unclear. Budding yeast (*S. cerevisiae*) expresses 14 different Hsp70 paralogs, five of which are localized to specific organelles [12]. Out of the remaining 9 cytosolic Hsp70s, 4 are from the Stress Seventy sub-family A (SSA) comprised of Ssa1, 2, 3 and 4 [12–16]. Previously, Hsp70 paralogs were thought to be functionally indistinguishable apart from spatiotemporal expression patterns, however recent findings suggest unique functions for Ssa paralogs [12,13].

Ssa paralogs arose from genome duplication and are highly conserved, with Ssa1 sharing 99%, 84% and 85% amino acid identity with Ssa2, 3 and 4, respectively [12]. The most prominent difference between the Ssa1-4 paralogs is their expression levels; Ssa1/2 are expressed constitutively at high levels whereas Ssa3/4 are only expressed during cell stress [12,17–21]. Although yeast can survive on the loss of any of 3 Ssas if the 4th is expressed at high levels, the phenotypes of these cells vary in terms of heat resistance longevity, ability to fold certain clients [22–25].

In this study, in order to better understand functional differences between Ssa1-4, we utilized the model chaperone client Ribonucleotide Reductase (RNR). RNR is an enzyme that is important for the production of deoxyribonucleotides (dNTPs) which are used in DNA synthesis and repair [26]. RNR is comprised of two diverse subunits, the large subunit R1 (R1 in vertebrates, Rnr1/Rnr3 in yeast) which contains the allosteric regulatory sites [27] and the small subunit R2 (R2/R2B in vertebrates, Rnr2/Rnr4 in yeast) which consists of a cell cycle regulated binuclear iron center and a tyrosyl free radical [28–32]. Due to its crucial role in the maintenance of genome integrity and subsequently cell survival, RNR remains an attractive anticancer target [29,31,33]. Several RNR inhibitors have been developed and used in a clinical setting including hydroxyurea (HU), triapine and gemcitabine [29,34–36].

Previous studies in both yeast and mammalian cells have identified Hsp70 as an important regulator of RNR with small molecule chaperone inhibitors such as 17-AAG promoting RNR subunit degradation [37–39]. Hsp70 inhibition sensitizes cancer cells to gemcitabine and the combination of Hsp70 and RNR inhibitors has the potential to form the basis of a novel anti-

cancer therapeutic [37–42]. Recently, the Hsp70 co-chaperone Ydj1/DNAJA1 (yeast/mammalian) was identified to assist Hsp70 in the regulation of RNR. Lack of Ydj1 in *S. cerevisiae* results in reduced Rnr2 subunit expression and stability against degradation [38,39]. This interaction was found to be conserved in humans, where DNAJA1 and R2B assist in RNR complex stability and activity in mammalian cells [38,39]. Additionally, inhibition of DNAJA1 with 116-9e, a small molecule inhibitor that blocks Hsp40 binding to Hsp70 through the J-domain resulted in disruption of R2B-DNAJA1 interaction and sensitized cells to HU and triapine [38,39].

Here we characterize the relative roles of Ssa1, 2, 3, and 4 in regulating ribonucleotide reductase in yeast. We reveal that yeast expressing single Ssas as their sole cytosolic Hsp70 on identical promoters display differing abilities to respond to DNA damaging agents. This can be explained by the loss of RNR subunit stability, occurring due to decreased Ssa-RNR interaction. Finally, we provide evidence that the C-terminal domain of Hsp70 is responsible for selectivity in activating RNR.

Results

Ssa paralogs contribute differentially to the resistance to DNA-perturbing agents and the transcriptional response to DNA damage

Previous studies have demonstrated a critical role for Hsp70 and Hsp90 in supporting RNR activity in yeast and mammalian cells [37–39]. In order to dissect the unique roles of the yeast Hsp70 paralogs Ssa1-4 in supporting the DNA damage response (DDR), we screened cells expressing either Ssa1, 2, 3 or 4 (under the constitutive Ssa2 promoter) as the sole cytosolic Hsp70 for growth against various DNA damaging agents including hydroxyurea (HU), 5-fluorouracil (5-FU), hydrogen peroxide (H_2O_2) and methyl methanesulfonate (MMS) (Fig 1A–1D). Yeast expressing Ssa1 or Ssa2 were markedly more resistant to all DNA damaging agents compared to Ssa3 or Ssa4 cells (Fig 1A). Cells expressing Ssa3 or Ssa4 as their sole Ssa displayed an increased sensitivity to HU, 5-FU and H_2O_2 but not MMS (Fig 1A–1D). To determine whether this phenotypic difference was due to altered DNA damage response-regulated transcription, we compared induction of *RNR3* in HU-treated Ssa1, 2, 3 and 4 cells (Fig 1E). Consistent with the phenotypes in Fig 1, Ssa3 and Ssa4 cells were unable to fully activate DDR transcription, displaying a significant decrease in HU-mediated *RNR3* expression (Fig 1E).

Ribonucleotide reductase subunit levels are compromised in cells solely expressing either Ssa3 or Ssa4

Our previous studies described a role for Hsp70 function in maintaining an active RNR complex in yeast and human cells. To determine whether the inability of Ssa3/4 cells to grow in the presence of DNA-damaging agents could be explained by loss of RNR function, we queried the steady-state levels of Rnr1, Rnr2 and Rnr4 protein in cells expressing single Ssa paralogs. Although Rnr1 levels remained independent of Ssa1 paralog (Fig 2A), clear differences in Rnr2 and Rnr4 levels were observed (determined by normalizing RNR levels to a loading control of PGK1). Rnr2 levels in Ssa3/4 cells were significantly lowered in both untreated and treated conditions compared to cells whose primary Hsp70 was Ssa1 or Ssa2 (Fig 2B). In contrast, while Rnr4 levels in untreated conditions were independent of Ssa version, the levels of HU-induced Rnr4 expression were substantially decreased in Ssa3 or Ssa4 cells (Fig 2C).

The steady state level of proteins are carefully balanced by both rate of transcription and protein degradation. To determine whether the altered RNR subunit expression observed in Ssa3 and Ssa4 cells was a result of altered transcription, we quantified *RNR1*, *RNR2* and *RNR4*

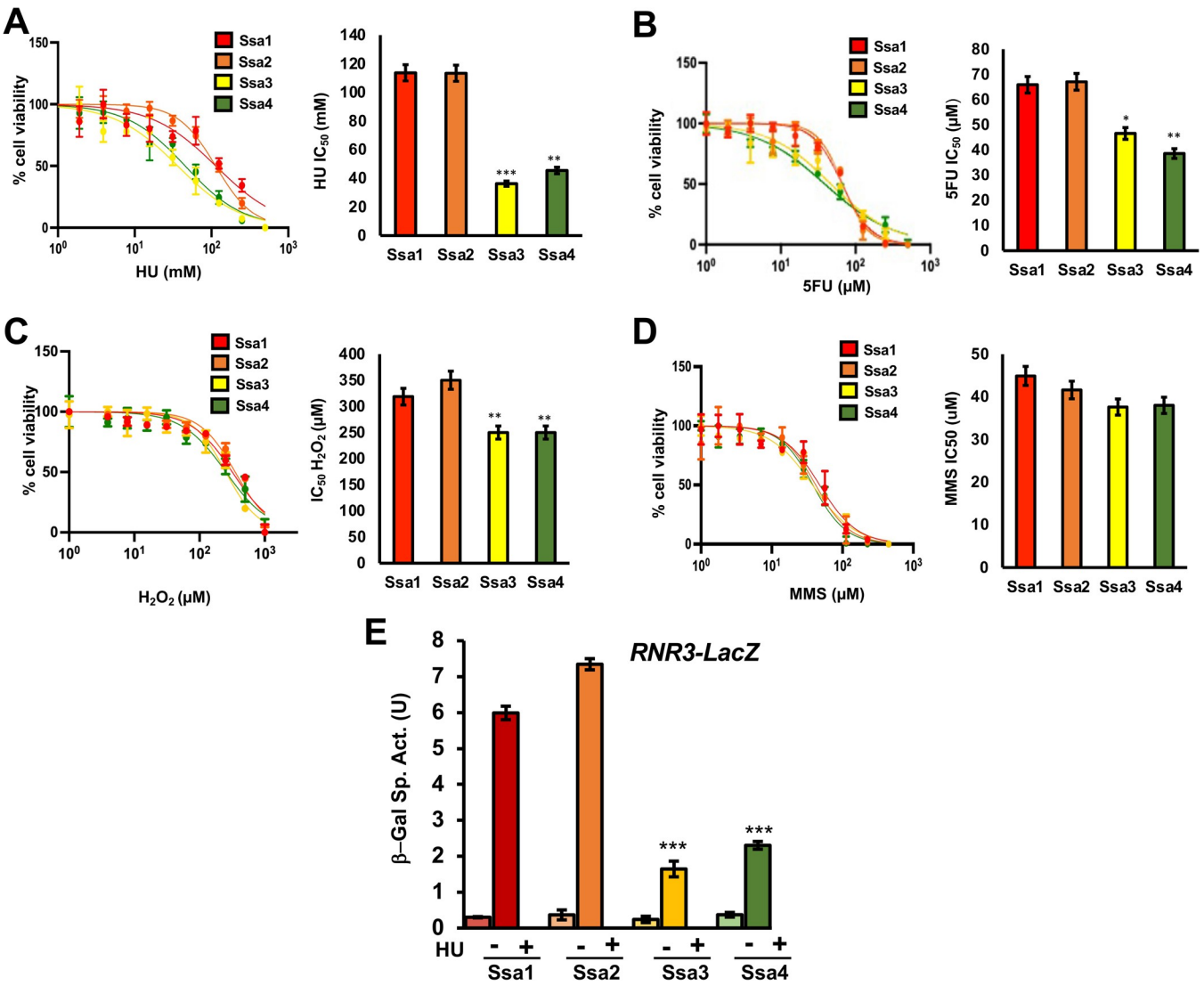

Fig 1. Ssa paralogs confer differential resistance to DNA-damaging agents. (A-D) mid-log *ssa1-4Δ* cells expressing either Ssa1, 2, 3 or 4 were treated with a serial dilution of the indicated drug in a 96-well format for 18 hrs. at which point yeast growth (OD600) was measured via plate reader. Each value represents the mean and standard deviation (error bar) from three independent transformants. Statistical significance were calculated via ANOVA. *, P≤0.05; **, P≤0.01; ***, P≤0.001 as compared to the Ssa2 strain. (E) An *RNR3-LacZ* reporter plasmid was transformed into the indicated yeast strains. Transformants were grown and subjected to either 0 or 200mM HU for 3 hours. β-Galactosidase activity was measured in crude extracts. β-Galactosidase specific activity [-Gal Sp. Act. (U)] is shown on the y axis. Each value represents the mean and standard deviation (error bar) from three independent transformants; *, P≤0.05**, P≤0.01; ***, P≤0.001 as compared to the Ssa2 strain.

https://doi.org/10.1371/journal.pgen.1010079.g001

mRNA expression in Ssa-paralog specific yeast using real-time quantitative polymerase chain reaction (RT-qPCR). *RNR1 and RNR2* transcription was independent of Ssa paralog, whereas HU-induced *RNR4* induction was compromised in cells expressing only Ssa3 and Ssa4 (Fig 3A). To determine whether the protein stability of Rnr1, Rnr2 and Rn4 had also been compromised in Ssa3 and Ssa4-expressing cells, we examined the half-life of RNR subunits by transcriptional shut-off experiments. While Rnr1 stability was independent of Ssa paralog, Rnr2 stability was substantially lowered in Ssa3/4 cells upon treatment with HU (Fig 3B). In contrast, Rnr4 stability was only decreased in Ssa3 cells (Fig 3B).

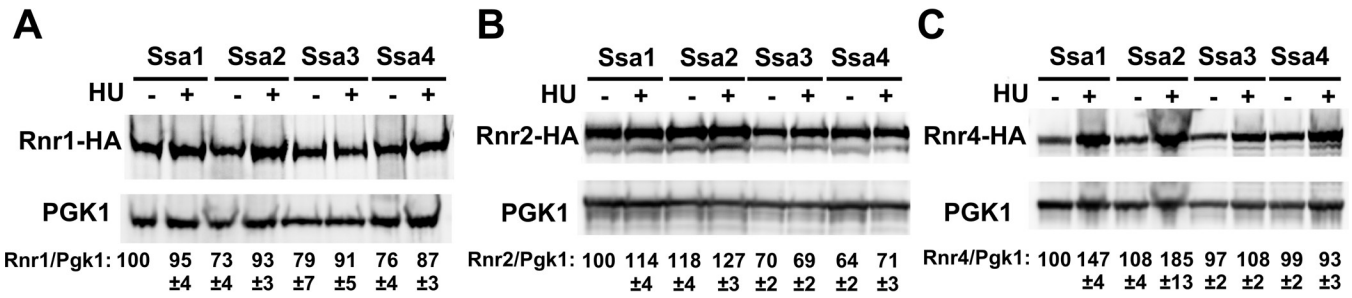

Fig 2. Steady-state levels of RNR small subunits are dependent on Ssa paralogs. *ssa1-4Δ* cells expressing either Ssa1, 2, 3 or 4 and endogenously tagged Rnr1-HA, Rnr2-HA or Rnr4-HA were grown to exponential phase and were either left untreated or were treated with 200mM HU for 3 hours. Cell extracts were obtained, resolved on SDS-PAGE gels and analyzed by immunoblotting with anti-HA and PGK1 antibodies. PGK1 was used as a loading control. The ratio of RNR subunit/PGK was quantified and determined from three replicate experiments.

https://doi.org/10.1371/journal.pgen.1010079.g002

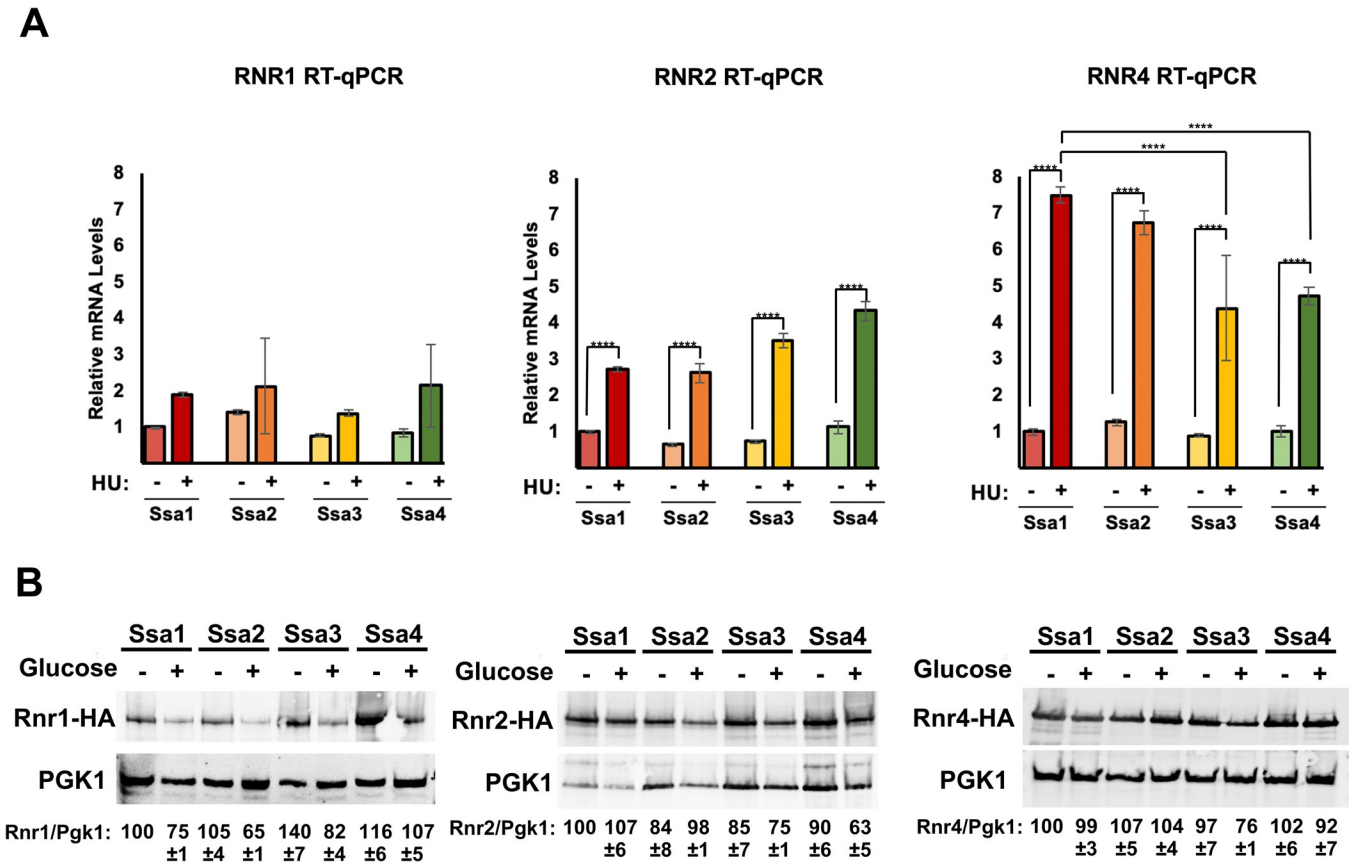

Fig 3. Transcription and stability of RNR subunits are altered in cells only expressing one Ssa paralog. (A) Quantitation of *RNR1*, *RNR2* and *RNR4* mRNA levels in Ssa1, 2,3 or 4-expressing yeast. Levels of *RNR1*, *RNR2* and *RNR4* mRNAs in Ssa1, 2,3 or 4 cells were determined by reverse transcription and RT-qPCR. Signals of *RNR1*, *RNR2* and *RNR4* were normalized against that of *ACT1* in each strain, and the resulting ratios in Ssa1 cells were arbitrarily defined as onefold. Data are the average and SD from three replicates *, P≤0.05**, P≤0.01; ***, P≤0.001; ****, P≤0.0001 as compared to indicated strains. (B) RNR subunit stability in yeast expressing single Ssa paralogs. Ssa1, 2,3 or 4-expressing cells transformed with either pGAL1-HA-Rnr1, 2 or 4 plasmids were grown to mid-log phase in YP Galactose medium. RNR expression was shut off by addition of 2% glucose to cultures. Cell lysates from these samples were analyzed over time by Western Blotting for the stability of HA-RNR subunit (HA antibody) and loading control (PGK1). The ratio of RNR/PGK was quantified and determined from three biological replicate experiments.

https://doi.org/10.1371/journal.pgen.1010079.g003

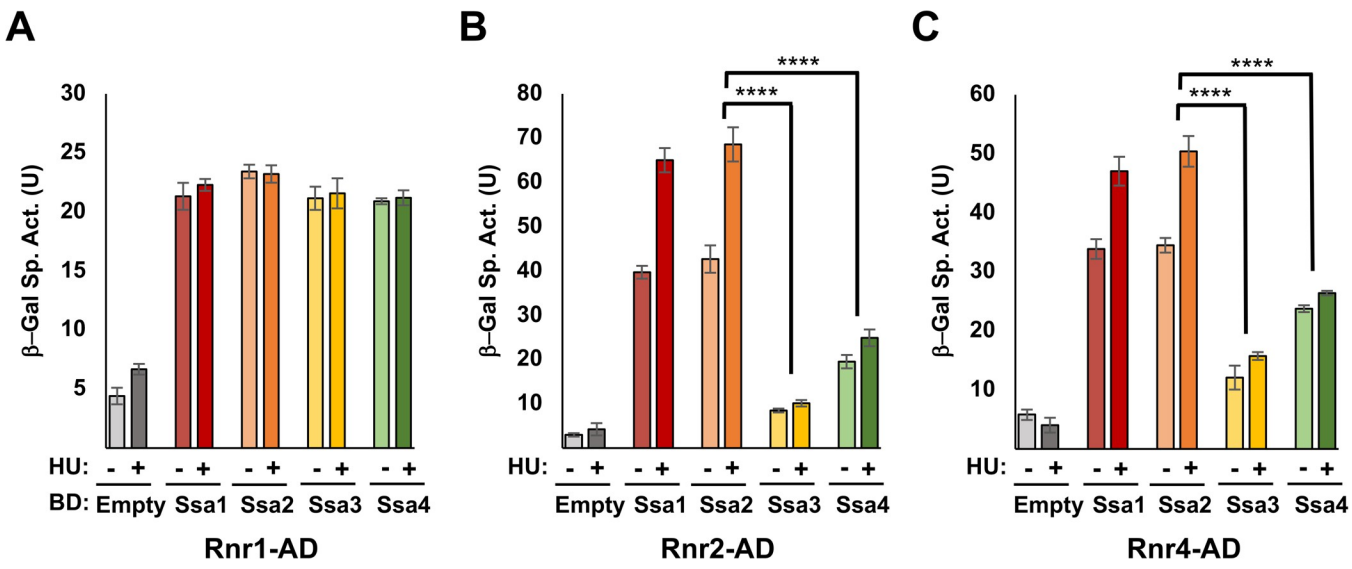

Fig 4. RNR small subunits display binding selectivity for Ssa paralogs. PJ694a/α cells were transformed with the appropriate AD-RNR and BD-Ssa fusions. Cells were grown in selective media to the mid-log phase at which point protein was extracted and analyzed for β-galactosidase activity. Each value represents the mean and standard deviation (error bar) from three independent transformants. Statistical significance between samples was calculated as above. *, P≤0.05**, P≤0.01; ***, P≤0.001; ****, P≤0.0001 compared to indicated strains.

https://doi.org/10.1371/journal.pgen.1010079.g004

RNR subunits display a binding preference for Ssa1 and Ssa2

Hsp90, Hsp70 and Hsp40 proteins in yeast and mammalian cells bind RNR subunit components [37–39]. In order to determine if the observed RNR instability in Ssa3/4 cells was a consequence of decreased RNR-chaperone interaction, we assessed the physical interaction of Rnr1, Rnr2 and Rnr4 proteins with Ssa1, 2, 3, and 4 by yeast two-hybrid analysis. In both experiments, Rnr1 interacted equally with all four Ssas (Fig 4A), whereas both Rnr2 and Rnr4 displayed a clear binding preference for Ssa1 and Ssa2 (Fig 4B and 4C).

RNR-Ydj1 interaction is weaker in cells solely expressing Ssa3 or Ssa4

Recent studies have revealed that Hsp70 paralogs display differing affinities for their associated co-chaperones [25,43]. In light of our previous work indicating that Ydj1 directly regulates RNR activity [38], we sought to determine whether Ydj1 association with RNR was reduced in Ssa3/4-expressing cells. We immunoprecipitated HA-tagged Rnr1, Rnr2 or Rnr4 from Ssa1, Ssa2, Ssa3 or Ssa4 cells and assessed the association of Ydj1 via Western Blotting. Ydj1 interacted with Rnr1 equally in Ssa1-4 cells in both unstressed and HU-treated cells (Fig 5A). Interestingly, both Ydj1-Rnr2 and Ydj1-Rnr4 interaction decreased in cells solely expressing Ssa3 and Ssa4 (Fig 5B and 5C).

The SBDβ and CTD regions of Ssa2 (542–639) are required for full RNR activity

Hsp70 is comprised of 3 major domains, NBD, SBD and CTD, the first of which is connected to the last two via a flexible linker. Ssa2 and Ssa4 share 84% sequence similarity with the end of the SBD and entirety of the CTD being the least conserved (Fig 6A and 6B). To understand the origin of the functional difference between the Ssa2 and Ssa4 in regard to RNR function we created Ssa2-Ssa4 chimeras based on these regions previously delineated in [13] and assessed their resistance to media containing HU. The Ssa24 construct consists of amino acids (a.a.)

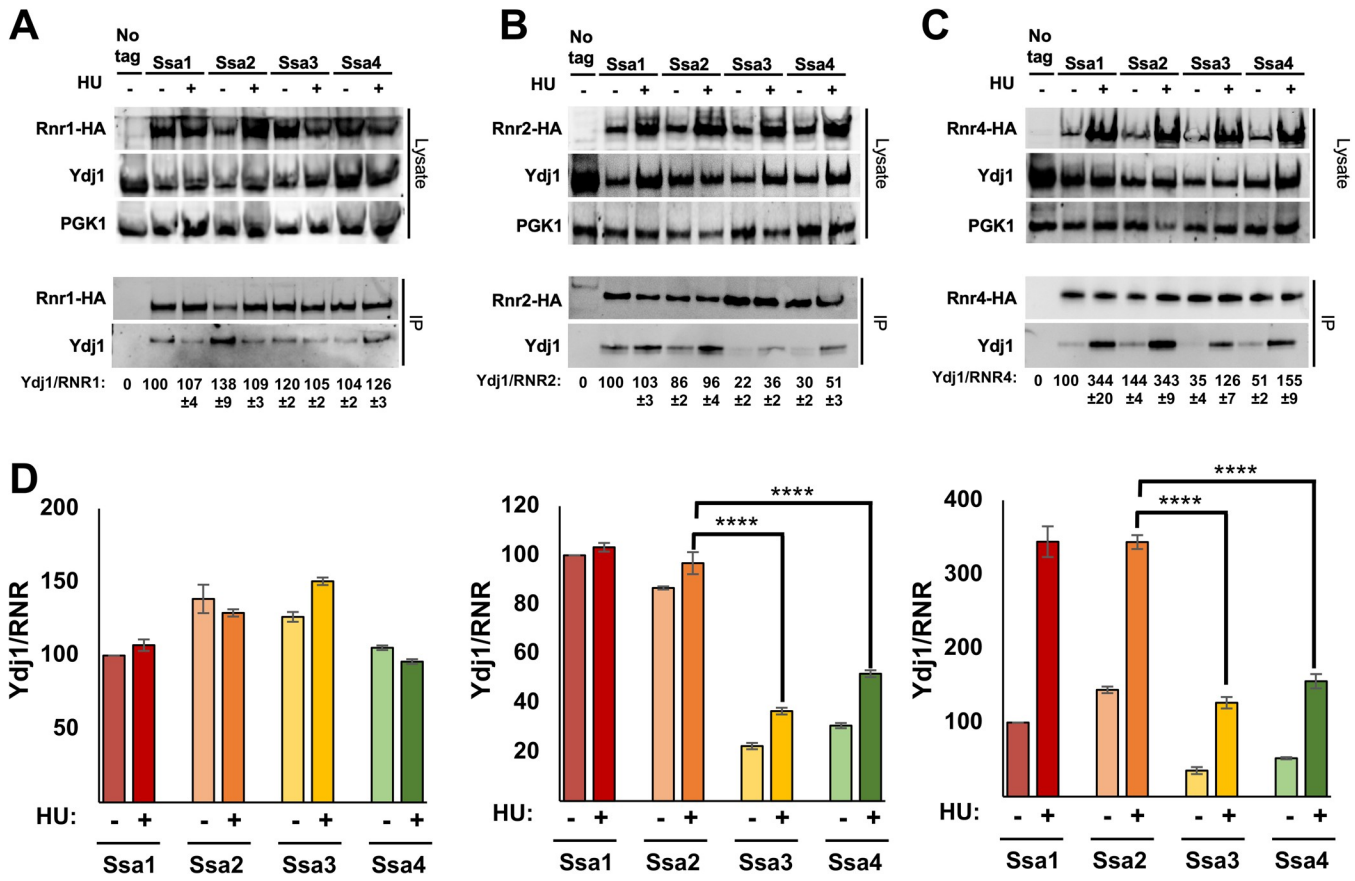

Fig 5. Small RNR subunit interaction with Ydj1 is decreased in Ssa3 and Ssa4 cells. (A-C) Cells expressing either Ssa1, 2, 3 or 4 as their sole Ssa and HA-tagged Rnr1/Rnr2/Rnr4 were grown to exponential phase and were either left untreated or were treated with 200 mM HU for 3 hrs. HA-RNR complexes were immunoprecipitated with anti-HA magnetic beads and were subjected to SDS-PAGE and analyzed by immunoblotting with anti-HA antibodies to detect the RNR subunits or anti-Ydj1 antibodies to detect Ydj1. (D) Interaction between RNR and Ydj1 (Ydj1/RNR) was calculated by quantitating bands from three replicate experiment. Each value represents the mean ± SD (n = 3). Statistical significance between samples was calculated ANOVA. $P \leq 0.05^{**}$, $P \leq 0.01$; ***, $P \leq 0.001$; ****, $P \leq 0.0001$ compared to indicated strains.

https://doi.org/10.1371/journal.pgen.1010079.g005

1–542 of Ssa2 fused to a.a. 543–639 of Ssa4 and vice-versa for the Ssa42 construct. Although yeast expressing the Ssa42 was as resistant to HU as Ssa4 cells, Ssa24 cells phenocopied Ssa4 cells (Fig 6C). In an effort to determine whether the a.a. region 1–542 of Ssa2 controlled the transcriptional output of the DNA damage response, we compared expression of β-galactosidase driven by a DNA-damage responsive promoter (*RNR3* promoter-lacZ) in HU-treated cells expressing Ssa2, Ssa4, Ssa24 and Ssa42. In correlation with the previous result, Ssa24 cells were unable to fully activate *RNR3* transcription (Fig 6D). Taken together these results suggest the amino acids 542–639 of the Ssas are critical for full RNR activity and thus the cellular response to HU.

Discussion

A fundamental mystery in molecular chaperone research is why cells express so many apparently similar and functionally redundant chaperone paralogs. Historically, it was generally thought that the main differences were in their expression across cells and tissues where the constitutive Hsp70 performed general housekeeping duties and the inducible form protected cells against environmental stress. However, several recent studies have shown that even when

chaperone paralogs are expressed in yeast at equivalent levels as the sole cytosolic Hsp70, these cells display dramatically different phenotypes [23–25,44–46].

A challenge in understanding the differential role of the Ssa paralogs is a lack of verified client proteins. While several Hsp70 interactomes have been published under differing conditions and phosphorylation site mutations, validation of these and their cellular effect is still under investigation [37,47–51]. Excellent attempts to dissect the roles of Ssa paralogs include the well-established Hsp90 client (Ste11) and a non-yeast client, v-Src in addition to the yeast prions [*URE3*] and [PSI^+] [23,25,52,53]. In our previous studies, we managed to identify Hsp90, Hsp70 and Hsp40 as key regulators of RNR in yeast and humans [39], providing an ideal system in which to further probe SSA isoform-specific differences.

In this study, we observed distinct differences in the ability of yeast expressing single SSA paralogs to survive insults to their genome integrity. Ssa1 and Ssa2-expressing cells were more resistant to HU, 5-FU and H_2O_2 than Ssa3 or Ssa4 cells. It is interesting to note that despite the above differences, there appeared to be no difference in the response to MMS between paralogs. This result may reflect the different kinds of DNA damage that these agents inflict on DNA. HU, 5-FU and H_2O_2 act primarily by causing single-strand damage and replication stress as opposed to MMS which acts to cause double-strand breaks.

Hsp70 and its corresponding co-chaperone Ydj1 have been shown to play a role in the stabilization of the RNR subunits in both yeast and human cells [38, 39]. In this study, we observed decreased Rnr2 levels and a lack of HU-inducibility of Rnr4 in Ssa3 and Ssa4-expressing cells. Further dissection of this phenomenon revealed that the lowered levels of Rnr2 were primarily due to increased subunit instability as determined by the promoter shut-off experiments. In contrast, the altered levels of Rnr4 in Ssa3/4 cells were a combination of transcriptional and protein stability effects. The lowered transcription of Rnr4 may be a consequence of altered DDR signaling, especially as RNR levels are directly controlled by the activity of Mec1, Tel1, Rad53 and Rad9, the latter of which is an Ssa1/2 client [54]. It is thus possible that in cells lacking Ssa1 and 2, Rad9 is destabilized leading to an inability to activate DDR and induce Rnr4 expression. While future studies on Ssa paralog interaction with main components of DDR signaling may be informative, our yeast two-hybrid experiments clearly show that Rnr2 and Rnr4 have a binding preference for Ssa1 and Ssa2 compared to their inducible counterparts. Given the amino acid conservation between the four paralogs, such a binding difference is rather striking. Clients of chaperones are processed via their co-chaperones and given that Ydj1 is key for RNR activity, we considered the possibility that paralog-specific binding of RNR subunits may be mediated via Ydj1. Our data in Fig 5 clearly shows this to be the case as Ydj1 interaction with Rnr2 and Rnr4 is decreased in Ssa3/4 cells.

Identifying regions of Hsp70 that determine client specificity remains challenging considering the essential nature of the protein and sequence similarity. Hsp70 is comprised of a nucleotide binding domain (NBD) which is important for co-chaperone binding and ATPase activity, a substrate binding domain (SBD) which is important for client interaction and a C-terminal domain (CTD) that binds co-chaperones [2]. Out of the four Ssa paralogs, Ssa2 cells are the most resistant to DNA damaging agents including HU, while Ssa4 cells are the most sensitive. In order to further dissect the of the sequence determinants for HU resistance, we used Ssa2-Ssa4 chimeras. Interestingly yeast expressing a chimera consisting of the a.a. 1–542 of Ssa2 and the a.a. 542–639 of Ssa4 (Ssa24) was sensitive to HU, pinpointing the CTD domain of Ssa2 as being key for RNR function and resistance to genome perturbing agents. The highest sequence variation between Ssa2 and Ssa4 occurs towards the end of the SBD (specifically the outer-facing region of the "lid") and the unstructured CTD (see Fig 6). Previous studies have identified this region as being important for the binding of co-chaperone proteins. The VEEVD sequence at the end of Hsp70/Ssa1 is critical for interaction with DNAJB-type co-

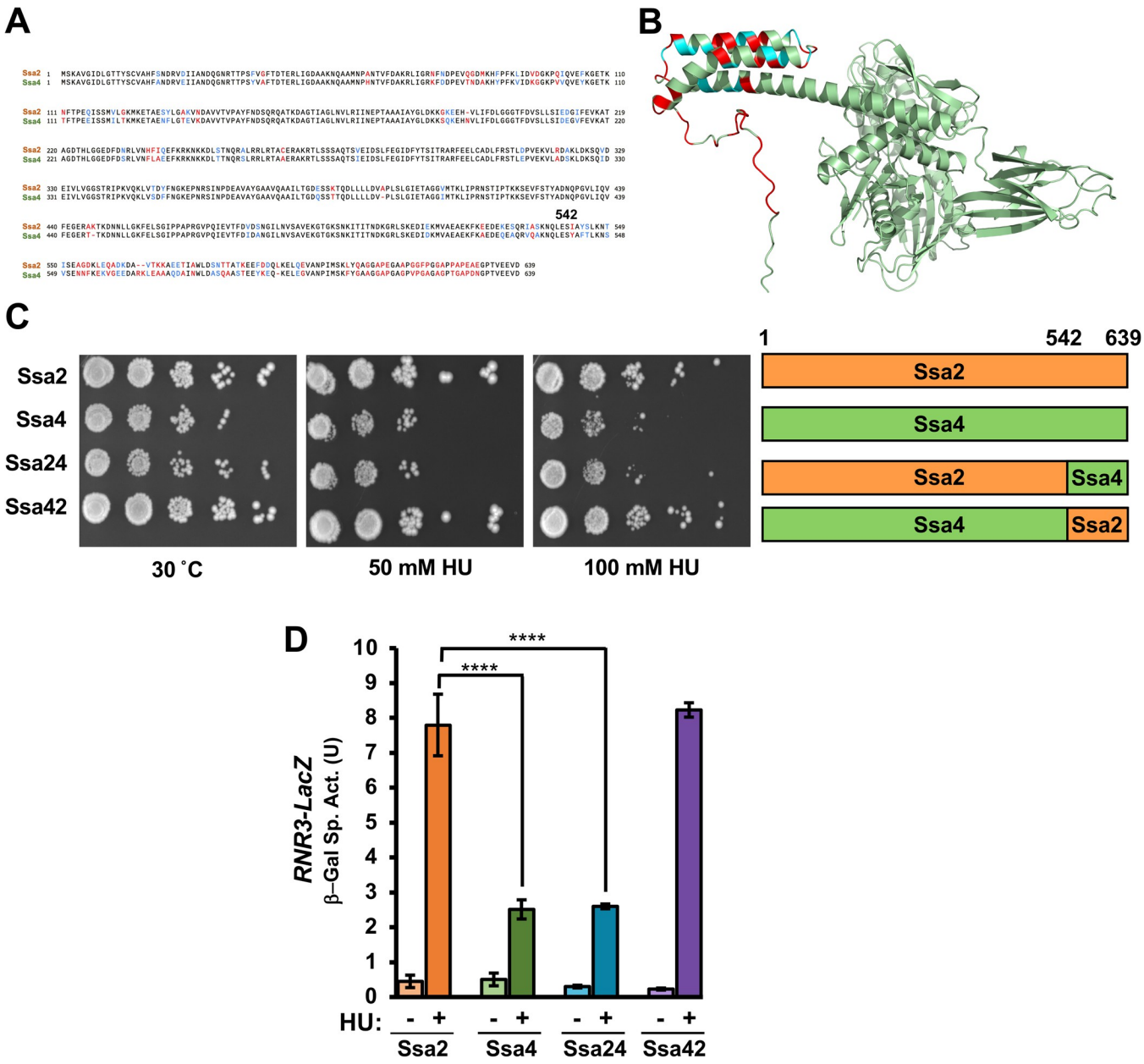

Fig 6. The C-terminus of Ssa2 is required for HU resistance. (A) Sequence alignment between Ssa2 and Ssa4 was created using Clustal Omega. Amino acids are labeled either Black (identical), Blue (similar) or Red (different). (B) Areas of sequence variance between Ssa2 and Ssa4 mapped to the predicted structure for Ssa2. The structure of Ssa2 was modeled via AlphaFold and rendered in PyMol. Residue similarity between Ssa2 and 4 was denoted by color (green, identical; blue similar; red, different). (C) Chimeras of Ssa2 and Ssa4 display altered resistance to hydroxyurea. Cells expressing either Ssa2, 4, 24 or 42 as the sole Ssa were grown overnight to saturation and serial 10-fold dilutions were plated by pin plating from 96-well plates onto YPD alone or YPD containing Hydroxyurea. Plates were imaged after 3 days. (D) DNA-damage response transcription in Ssa2-4 chimeras. An *RNR3-LacZ* reporter plasmid was transformed into the indicated yeast strains. Transformants were grown and subjected to 0 or 200mM HU for 3 hours. β-Galactosidase activity was measured in crude extracts. β-Galactosidase specific activity (in units) [-Gal Sp. Act. (U)] is shown on the y axis. Each value represents the mean and standard deviation (error bar) from three independent transformants; P≤0.05**, P≤0.01; ***, P≤0.001; ****, P≤0.0001 compared to indicated strains.

https://doi.org/10.1371/journal.pgen.1010079.g006

chaperones including Sis1 [55–58]. However, there is also substantial evidence that the CTD is also important for the binding of Ydj1. Loss of the last 8 amino acids of Ssa1 substantially reduces the Ssa1-Ydj1 interaction [59] and a 20-amino acid motif in Ssa1 containing GGAP repeats was recently revealed to be necessary for Ssa1 to bind to Ydj1 and activate both the cell

integrity and heat shock responses [60]. These results parallel those seen with mammalian Hsp70 paralogs, where each paralog displays a clear binding preference for certain co-chaperones [43]. Taken together, our data suggest that the sequence variation in the CTD is primarily responsible for differential recruitment and folding of RNR small subunits. It is worth noting that recent studies have uncovered a non-canonical binding site in Hsp70 required for binding and folding of alpha-synuclein [61]. It is possible that this region and the area that determines RNR subunit binding heavily overlap. It is interesting to note that co-chaperones are thought to bind select clients first and present them to Hsp70 for folding. This provides rationale for why there are so many diverse but related co-chaperones in both yeast and mammalian cells. Our data clearly shows that Ydj1 interaction with RNR is altered in Ssa3 and 4 expressing cells. This suggests that Ydj1 may actually form a complex with Ssa1/2 prior to binding RNR. The reduced binding of Ssa3 and Ssa4 to RNR then would naturally result in reduced binding to Ydj1. Future studies to delineate the structure of the RNR-chaperone complex should resolve some of the fascinating questions. Studies over the past decade have identified numerous post-translational modifications (PTMs) on chaperones which are collectively known as the "Chaperone Code" [62–64]. This code modifies a variety of chaperone properties including localization, stability, and most importantly client and co-chaperone folding. Several PTMs have been identified in the C-terminal region of Hsp70. In future studies we hope to clarify the role of Hsp70 PTMs on interaction with RNR. Similarly, the data presented here and in our previous study clearly show that interaction between Ydj1 and RNR subunits are stress-induced [38]. It is conceivable that this interaction is also mediated by PTMs on either or both co-chaperone/RNR proteins. Taken together, our data demonstrates a clear role for Ssa1 and Ssa2 (but not Ssa3 or Ssa4) in the maturation and stability of RNR subunits. This makes cellular sense given that Ssa3 and 4 are present at very low levels in cells except in response to proteotoxic stress. RNR complex proteins in yeast exposed to any form of DNA damage at standard temperatures would thus only have access to Ssa1 and 2. It is possible then that the lack of selective pressure on Ssa3 and 4 to be required to bind housekeeping proteins like RNR for cell viability may have contributed to their sequence divergence from Ssa1 and Ssa2 over time. Molecular chaperones (and often their clients) are well-conserved throughout nature. We have previously shown that Hsp70 and Hsp40 also bind RNR subunits in mammalian cells [38,39]. We envisage future studies that probe this complex interaction in mammalian cells, possibly in the hope of identifying novel ways to inhibit RNR in cancer, feasible given the role of DNAJA1 and other co-chaperones in anticancer drug resistance [65, 66]

Materials and methods

Yeast Strains and growth conditions

Yeast cultures were grown in either YPD (1% yeast extract, 2% glucose, 2% peptone) or grown in SD (0.67% yeast nitrogen base without amino acids and carbohydrates, 2% glucose) supplemented with the appropriate nutrients to select for plasmids and tagged genes. Escherichia coli DH5α was used to propagate all plasmids. E. coli cells were cultured in Luria broth medium (1% Bacto tryptone, 0.5% Bacto yeast extract, 1% NaCl) and transformed to ampicillin resistance by standard methods. Hsp70 isoform plasmids pRS315P_{SSA2}-SSA1, pRS315P_{SSA2}-SSA2, pRS315P_{SSA2}-SSA3, pRS315P_{SSA2}-SSA4 [67] were transformed into yeast strain *ssa1–4*Δ [68] using PEG/lithium acetate. After restreaking onto media lacking leucine, transformants were streaked again onto media lacking leucine and containing 5-fluoro-orotic acid (5-FOA), resulting in yeast that expressed Hsp70 paralogs as the sole cytoplasmic Hsp70 in the cell.

For tagging the genomic copy of *RNR1*, *RNR2* and *RNR4* with a HA epitope at the carboxy-terminus, the pFA6a-HA-His3MX6 plasmid was used in a manner similar to [38]. A full table

of yeast strains and plasmids that were used can be found in Tables A and B in S1 File. For serial dilutions, cells were grown to mid-log phase, 10-fold serially diluted and then plated onto appropriate media using a 48-pin replica-plating tool. Images of plates were taken after 3 days at 30˚C. 200mM HU was used for serial dilutions and to stress yeast cells, a concentration established in Tkach et al. [69].

For IC_{50} calculations, cells were grown to mid-log phase, diluted in a sterile 96 well plate in media containing HU, 5-FU, H_2O_2, MMS and were 10-fold serially diluted at indicated concentrations. Cells were continuously shaken for 24 hours at 30˚C and the optical density of the reaction was measured at 600nm. The mean and standard deviation from three independent transformants were calculated.

β-Galactosidase assays

For *RNR3-lacZ* fusion expression experiments, *ssa1-4Δ* yeast cells expressing single Ssa constructs or Ssa2/4 fusions were grown overnight in SD-URA media at 30˚C and then re-inoculated at OD600 of 0.2–0.4 and then grown for a further 4 hours. Cells were treated with 150 mM or 200 mM HU for 3 hours and then RNR3- lacZ fusion assays were carried out as described previously in Truman et al. [70]. Briefly, protein was extracted through bead beating and protein was quantitated via Bradford assay. The beta-Galactosidase reaction containing 50 μg of protein extract in 1 ml Z-Buffer (30) was initiated by addition of 200 μl ONPG (4 mg/ml) and incubated at 28˚C until the appearance of a pale-yellow color was noted. The reaction was quenched via the addition of 500 μl Na2CO3 (1M) solution. The optical density of the reaction was measured at 420nm. β-Gal activity was calculated using ((OD420 x 1.7)/(0.0045 x protein x reaction time)), where protein is measured in mg, and time is in minutes. The mean and standard deviation from three independent transformants were calculated.

Galactose promoter shut-off experiments

Ssa1-4Δ yeast cells expressing either Ssa1, 2, 3 or 4 as the sole Hsp70 isoform were transformed with either pGAL1-HA-Rnr1, 2 or 4 plasmids were grown to mid-log phase in YP Gal medium (1% yeast extract, 2% galactose, 2% peptone). Transcription of pGAL1-HA-Rnr1, 2 or 4 was shut off by the addition of 2% glucose to cultures. Aliquots of cells were collected at 0 and 4 hours after the addition of glucose. Cell lysates from these samples were analyzed by Western Blotting for stability of RNR subunit (HA antibody) and loading control (PGK1).

Western blotting

Protein extracts were made as described and 20 μg of protein was separated by 4%–12% NuPAGE SDS-PAGE (Thermo) [48]. Proteins were detected using the following antibodies; anti-HA tag (Thermo #26183), Anti-FLAG tag (Sigma, #F1365), anti-PGK1 (Thermo # PA5-28612), anti-Ydj1 (StressMarq #SMC-166D). Blots were imaged on a ChemiDoc MP imaging system (Bio-Rad). After treatment with SuperSignal West Pico Chemiluminescent Substrate (GE). Blots were stripped and re-probed with the relevant antibodies using Restore Western Blot Stripping Buffer (Thermo).

Purification of HA-tagged Rnr1, 2 and 4 from yeast

Ssa1-4Δ yeast cells expressing genomically-tagged HA-Rnr1, Rnr2 and Rnr4 were transformed with Ssa1-4 pRS315 plasmids were grown overnight in SD-LEU media, and then reinoculated into a larger culture of selectable media and grown to an OD600 of 0.800. The cells were then either unstressed or stressed with 200 mM HU for four hours. Cells were harvested and HA-

tagged proteins were isolated as follows: Protein was extracted via bead beating in 500 μl binding buffer (50 mM Na-phosphate pH 8.0, 300 mM NaCl, 0.01% Tween-20). 200 μg of protein extract was incubated with 30 μl anti-HA magnetic beads (Sigma) at 4˚C overnight. Anti-HA beads were collected by magnet then washed 5 times with 500 μl binding buffer. After the final wash, the buffer was aspirated and beads were incubated with 65 μl Elution buffer (binding buffer supplemented with 10 μg/ml 3X HA peptide (Apex Bio)) for 1 hour at 4˚ C, then beads were collected via magnet. The supernatant containing purified HA-RNR1, 2, and 4 were transferred to a fresh tube, 25 μl of 5x SDS-PAGE sample buffer was added and the sample was denatured for 5 min at 95˚ C. 20 μl of sample was analyzed by SDS-PAGE.

Quantitation of yeast RNR subunit transcription

Quantitation of yeast *RNR* transcription was carried out as in Zhang et al. [71]. Briefly, *Ssa1-4Δ* yeast cells expressing unique Ssas were grown overnight in YPD media at 30˚C, re-inoculated at OD600 of 0.2–0.4 and then grown for a further 4 hours. Cells were treated with 200 mM for 2 hours and total RNA was extracted from cells using a GeneJet RNA extraction kit. Total RNA (1 μg) was treated with 10 units of RNase-free DNase I (Thermo) for 30 min at 37˚C to remove contaminating DNA. DNAse I activity was stopped by adding 1 μL of 50 mM EDTA and incubating at 65˚C for 10 minutes. cDNA synthesis was carried out by iScript reverse transcriptase (BioRad) on aliquots of 1 μg RNA. The single-stranded cDNA products were used in qPCR on an ABI Fast 2000 real-time PCR detection system based on SYBR Green fluorescence. Sequences of oligo pairs (same as used in [71]) are listed in Table C in S1 File. Signals of *RNR1*, *RNR2* and *RNR4* were normalized against that of *ACT1* in each strain and the resulting ratios in WT cells were defined as onefold.

Yeast two hybrid analysis

Ssa1-4Δ cells expressing unique Ssas were transformed with the appropriate GAL4 AD and BD fusion proteins. Interaction between Ssa paralogs and RNR subunits was measured via β-galactosidase assays as in [70].

Supporting information

S1 File. List of all yeast strains, plasmids and primers used in this study. Table A. Yeast Strains Used in This Study. Table B. Plasmids Used in This Study. Table C. RT PCR Primers Used in This Study.
(DOCX)

Acknowledgments

We would like to thank Deepak Sharma and Daniel Masison for their reagents and advice on this work and Tawanda Zininga for his feedback on the preprint version of this manuscript.

Author Contributions

Conceptualization: Laura E. Knighton, Nitika, Andrew W. Truman.

Data curation: Laura E. Knighton, Siddhi Omkar, Andrew W. Truman.

Formal analysis: Siddhi Omkar, Andrew W. Truman.

Funding acquisition: Andrew W. Truman.

Investigation: Nitika, Andrew W. Truman.

Methodology: Laura E. Knighton, Nitika.

Resources: Andrew W. Truman.

Supervision: Laura E. Knighton, Andrew W. Truman.

Writing – original draft: Laura E. Knighton, Nitika, Andrew W. Truman.

Writing – review & editing: Laura E. Knighton, Nitika, Siddhi Omkar, Andrew W. Truman.

References

1. Nillegoda NB, Wentink AS, Bukau B. Protein Disaggregation in Multicellular Organisms. Trends Biochem Sci. 2018; 43(4):285–300. Epub 2018/03/05. https://doi.org/10.1016/j.tibs.2018.02.003 PMID: 29501325.
2. Rosenzweig R, Nillegoda NB, Mayer MP, Bukau B. The Hsp70 chaperone network. Nat Rev Mol Cell Biol. 2019; 20(11):665–80. Epub 2019/06/30. https://doi.org/10.1038/s41580-019-0133-3 PMID: 31253954.
3. Craig EA, Marszalek J. How Do J-Proteins Get Hsp70 to Do So Many Different Things? Trends Biochem Sci. 2017; 42(5):355–68. Epub 2017/03/21. https://doi.org/10.1016/j.tibs.2017.02.007 PMID: 28314505; PubMed Central PMCID: PMC5409888.
4. Kim YE, Hipp MS, Bracher A, Hayer-Hartl M, Hartl FU. Molecular chaperone functions in protein folding and proteostasis. Annual review of biochemistry. 2013; 82:323–55. Epub 2013/06/12. https://doi.org/10.1146/annurev-biochem-060208-092442 PMID: 23746257.
5. Kampinga HH, Craig EA. The HSP70 chaperone machinery: J proteins as drivers of functional specificity. Nat Rev Mol Cell Biol. 2010; 11(8):579–92. Epub 2010/07/24. https://doi.org/10.1038/nrm2941 PMID: 20651708; PubMed Central PMCID: PMC3003299.
6. Walsh P, Bursac D, Law YC, Cyr D, Lithgow T. The J-protein family: modulating protein assembly, disassembly and translocation. EMBO Rep. 2004; 5(6):567–71. Epub 2004/06/02. https://doi.org/10.1038/sj.embor.7400172 PMID: 15170475; PubMed Central PMCID: PMC1299080.
7. Balchin D, Hayer-Hartl M, Hartl FU. Recent advances in understanding catalysis of protein folding by molecular chaperones. FEBS Lett. 2020; 594(17):2770–81. Epub 2020/05/24. https://doi.org/10.1002/1873-3468.13844 PMID: 32446288.
8. Balchin D, Hayer-Hartl M, Hartl FU. In vivo aspects of protein folding and quality control. Science. 2016; 353(6294):aac4354. Epub 2016/07/02. https://doi.org/10.1126/science.aac4354 PMID: 27365453.
9. Assenza S, Sassi AS, Kellner R, Schuler B, De Los Rios P, Barducci A. Efficient conversion of chemical energy into mechanical work by Hsp70 chaperones. Elife. 2019; 8. Epub 2019/12/18. https://doi.org/10.7554/eLife.48491 PMID: 31845888; PubMed Central PMCID: PMC7000219.
10. Kellner R, Hofmann H, Barducci A, Wunderlich B, Nettels D, Schuler B. Single-molecule spectroscopy reveals chaperone-mediated expansion of substrate protein. Proc Natl Acad Sci U S A. 2014; 111(37):13355–60. Epub 2014/08/29. https://doi.org/10.1073/pnas.1407086111 PMID: 25165400; PubMed Central PMCID: PMC4169939.
11. Sekhar A, Rosenzweig R, Bouvignies G, Kay LE. Mapping the conformation of a client protein through the Hsp70 functional cycle. Proc Natl Acad Sci U S A. 2015; 112(33):10395–400. Epub 2015/08/05. https://doi.org/10.1073/pnas.1508504112 PMID: 26240333; PubMed Central PMCID: PMC4547247.
12. Lotz SK, Knighton LE, Nitika, Jones GW, Truman AW. Not quite the SSAme: unique roles for the yeast cytosolic Hsp70s. Curr Genet. 2019; 65(5):1127–34. Epub 2019/04/26. https://doi.org/10.1007/s00294-019-00978-8 PMID: 31020385; PubMed Central PMCID: PMC7262668.
13. Gaur D, Singh P, Guleria J, Gupta A, Kaur S, Sharma D. The Yeast Hsp70 Co-chaperone Ydj1 Regulates Functional Distinction of Ssa Hsp70s in the Hsp90 Chaperoning Pathway. Genetics. 2020. Epub 2020/04/18. https://doi.org/10.1534/genetics.120.303190 PMID: 32299842.
14. Hageman J, van Waarde MA, Zylicz A, Walerych D, Kampinga HH. The diverse members of the mammalian HSP70 machine show distinct chaperone-like activities. Biochem J. 2011; 435(1):127–42. Epub 2011/01/15. https://doi.org/10.1042/BJ20101247 PMID: 21231916.
15. Mayer MP. Intra-molecular pathways of allosteric control in Hsp70s. Philosophical transactions of the Royal Society of London Series B, Biological sciences. 2018; 373(1749). Epub 2018/05/08. https://doi.org/10.1098/rstb.2017.0183 PMID: 29735737; PubMed Central PMCID: PMC5941178.
16. Mayer MP, Bukau B. Hsp70 chaperones: cellular functions and molecular mechanism. Cellular and molecular life sciences: CMLS. 2005; 62(6):670–84. Epub 2005/03/17. https://doi.org/10.1007/s00018-004-4464-6 PMID: 15770419; PubMed Central PMCID: PMC2773841.

17. Werner-Washburne M, Stone DE, Craig EA. Complex interactions among members of an essential subfamily of hsp70 genes in Saccharomyces cerevisiae. Mol Cell Biol. 1987; 7(7):2568–77. Epub 1987/07/01. https://doi.org/10.1128/mcb.7.7.2568-2577.1987 PMID: 3302682; PubMed Central PMCID: PMC365392.

18. Werner-Washburne M, Craig EA. Expression of members of the Saccharomyces cerevisiae hsp70 multigene family. Genome. 1989; 31(2):684–9. Epub 1989/01/01. https://doi.org/10.1139/g89-125 PMID: 2698838.

19. Werner-Washburne M, Becker J, Kosic-Smithers J, Craig EA. Yeast Hsp70 RNA levels vary in response to the physiological status of the cell. J Bacteriol. 1989; 171(5):2680–8. Epub 1989/05/01. https://doi.org/10.1128/jb.171.5.2680-2688.1989 PMID: 2651414; PubMed Central PMCID: PMC209952.

20. Boorstein WR, Craig EA. Structure and regulation of the SSA4 HSP70 gene of Saccharomyces cerevisiae. J Biol Chem. 1990; 265(31):18912–21. Epub 1990/11/05. PMID: 2121731.

21. Boorstein WR, Craig EA. Transcriptional regulation of SSA3, an HSP70 gene from Saccharomyces cerevisiae. Mol Cell Biol. 1990; 10(6):3262–7. Epub 1990/06/01. https://doi.org/10.1128/mcb.10.6.3262-3267.1990 PMID: 2188113; PubMed Central PMCID: PMC360695.

22. Sharma D, Martineau CN, Le Dall MT, Reidy M, Masison DC, Kabani M. Function of SSA subfamily of Hsp70 within and across species varies widely in complementing Saccharomyces cerevisiae cell growth and prion propagation. PLoS One. 2009; 4(8):e6644. Epub 2009/08/15. https://doi.org/10.1371/journal.pone.0006644 PMID: 19680550; PubMed Central PMCID: PMC2721632.

23. Gupta A, Puri A, Singh P, Sonam S, Pandey R, Sharma D. The yeast stress inducible Ssa Hsp70 reduces alpha-synuclein toxicity by promoting its degradation through autophagy. PLoS Genet. 2018; 14(10):e1007751. Epub 2018/10/31. https://doi.org/10.1371/journal.pgen.1007751 PMID: 30376576; PubMed Central PMCID: PMC6226208.

24. Andersson R, Eisele-Burger AM, Hanzen S, Vielfort K, Oling D, Eisele F, et al. Differential role of cytosolic Hsp70s in longevity assurance and protein quality control. PLoS Genet. 2021; 17(1):e1008951. Epub 2021/01/12. https://doi.org/10.1371/journal.pgen.1008951 PMID: 33428620; PubMed Central PMCID: PMC7822560 following competing interests: D.O. and F.E. are employed by AstraZeneca Molndal, Sweden; S.H. is employed by Cochlear Nordic AB, Molnlycke, Sweden.

25. Gaur D, Singh P, Guleria J, Gupta A, Kaur S, Sharma D. The Yeast Hsp70 Cochaperone Ydj1 Regulates Functional Distinction of Ssa Hsp70s in the Hsp90 Chaperoning Pathway. Genetics. 2020; 215(3):683–98. Epub 2020/04/18. https://doi.org/10.1534/genetics.120.303190 PMID: 32299842; PubMed Central PMCID: PMC7337085.

26. Mikolaskova B, Jurcik M, Cipakova I, Kretova M, Chovanec M, Cipak L. Maintenance of genome stability: the unifying role of interconnections between the DNA damage response and RNA-processing pathways. Curr Genet. 2018; 64(5):971–83. Epub 2018/03/03. https://doi.org/10.1007/s00294-018-0819-7 PMID: 29497809.

27. Maicher A, Kupiec M. Rnr1's role in telomere elongation cannot be replaced by Rnr3: a role beyond dNTPs? Curr Genet. 2018; 64(3):547–50. Epub 2017/11/10. https://doi.org/10.1007/s00294-017-0779-3 PMID: 29119271.

28. Cerqueira NM, Pereira S, Fernandes PA, Ramos MJ. Overview of ribonucleotide reductase inhibitors: an appealing target in anti-tumour therapy. Current medicinal chemistry. 2005; 12(11):1283–94. Epub 2005/06/25. https://doi.org/10.2174/0929867054020981 PMID: 15974997.

29. Cerqueira NM, Fernandes PA, Ramos MJ. Ribonucleotide reductase: a critical enzyme for cancer chemotherapy and antiviral agents. Recent Pat Anticancer Drug Discov. 2007; 2(1):11–29. Epub 2008/01/29. https://doi.org/10.2174/157489207779561408 PMID: 18221051.

30. Chabes A, Domkin V, Larsson G, Liu A, Graslund A, Wijmenga S, et al. Yeast ribonucleotide reductase has a heterodimeric iron-radical-containing subunit. Proc Natl Acad Sci U S A. 2000; 97(6):2474–9. Epub 2000/03/16. https://doi.org/10.1073/pnas.97.6.2474 PMID: 10716984; PubMed Central PMCID: PMC15953.

31. Nordlund P, Reichard P. Ribonucleotide reductases. Annual review of biochemistry. 2006; 75:681–706. Epub 2006/06/08. https://doi.org/10.1146/annurev.biochem.75.103004.142443 PMID: 16756507.

32. Wang PJ, Chabes A, Casagrande R, Tian XC, Thelander L, Huffaker TC. Rnr4p, a novel ribonucleotide reductase small-subunit protein. Mol Cell Biol. 1997; 17(10):6114–21. Epub 1997/10/07. https://doi.org/10.1128/MCB.17.10.6114 PMID: 9315671; PubMed Central PMCID: PMC232461.

33. Mulder KW, Winkler GS, Timmers HT. DNA damage and replication stress induced transcription of RNR genes is dependent on the Ccr4-Not complex. Nucleic Acids Res. 2005; 33(19):6384–92. Epub 2005/11/09. https://doi.org/10.1093/nar/gki938 PMID: 16275785; PubMed Central PMCID: PMC1278945.

34. Singh A, Xu YJ. The Cell Killing Mechanisms of Hydroxyurea. Genes (Basel). 2016; 7(11). Epub 2016/11/22. https://doi.org/10.3390/genes7110099 PMID: 27869662; PubMed Central PMCID: PMC5126785.

35. Yarbro JW. Mechanism of action of hydroxyurea. Seminars in oncology. 1992; 19(3 Suppl 9):1–10. Epub 1992/06/01. PMID: 1641648.

36. Gandhi V, Plunkett W, Cortes JE. Omacetaxine: a protein translation inhibitor for treatment of chronic myelogenous leukemia. Clin Cancer Res. 2014; 20(7):1735–40. Epub 2014/02/07. https://doi.org/10.1158/1078-0432.CCR-13-1283 PMID: 24501394; PubMed Central PMCID: PMC4048124.

37. Truman AW, Kristjansdottir K, Wolfgeher D, Ricco N, Mayampurath A, Volchenboum SL, et al. Quantitative proteomics of the yeast Hsp70/Hsp90 interactomes during DNA damage reveal chaperone-dependent regulation of ribonucleotide reductase. Journal of proteomics. 2015; 112:285–300. Epub 2014/12/03. https://doi.org/10.1016/j.jprot.2014.09.028 PMID: 25452130; PubMed Central PMCID: PMC4485990.

38. Sluder IT, Nitika, Knighton LE, Truman AW. The Hsp70 co-chaperone Ydj1/HDJ2 regulates ribonucleotide reductase activity. PLoS Genet. 2018; 14(11):e1007462. Epub 2018/11/20. https://doi.org/10.1371/journal.pgen.1007462 PMID: 30452489; PubMed Central PMCID: PMC6277125.

39. Knighton LE, Delgado LE, Truman AW. Novel insights into molecular chaperone regulation of ribonucleotide reductase. Curr Genet. 2019; 65(2):477–82. Epub 2018/12/07. https://doi.org/10.1007/s00294-018-0916-7 PMID: 30519713; PubMed Central PMCID: PMC6421096.

40. Ghadban T, Dibbern JL, Reeh M, Miro JT, Tsui TY, Wellner U, et al. HSP90 is a promising target in gemcitabine and 5-fluorouracil resistant pancreatic cancer. Apoptosis. 2017; 22(3):369–80. Epub 2016/11/24. https://doi.org/10.1007/s10495-016-1332-4 PMID: 27878398.

41. Pedersen KS, Kim GP, Foster NR, Wang-Gillam A, Erlichman C, McWilliams RR. Phase II trial of gemcitabine and tanespimycin (17AAG) in metastatic pancreatic cancer: a Mayo Clinic Phase II Consortium study. Invest New Drugs. 2015; 33(4):963–8. Epub 2015/05/09. https://doi.org/10.1007/s10637-015-0246-2 PMID: 25952464; PubMed Central PMCID: PMC4905857.

42. Arlander SJ, Eapen AK, Vroman BT, McDonald RJ, Toft DO, Karnitz LM. Hsp90 inhibition depletes Chk1 and sensitizes tumor cells to replication stress. J Biol Chem. 2003; 278(52):52572–7. Epub 2003/10/23. https://doi.org/10.1074/jbc.M309054200 PMID: 14570880.

43. Serlidaki D, van Waarde M, Rohland L, Wentink AS, Dekker SL, Kamphuis MJ, et al. Functional diversity between HSP70 paralogs caused by variable interactions with specific co-chaperones. J Biol Chem. 2020; 295(21):7301–16. Epub 2020/04/15. https://doi.org/10.1074/jbc.RA119.012449 PMID: 32284329; PubMed Central PMCID: PMC7247296.

44. Waller SJ, Knighton LE, Crabtree LM, Perkins AL, Reitzel AM, Truman AW. Characterizing functional differences in sea anemone Hsp70 isoforms using budding yeast. Cell Stress Chaperones. 2018; 23(5):933–41. Epub 2018/04/27. https://doi.org/10.1007/s12192-018-0900-7 PMID: 29696514; PubMed Central PMCID: PMC6111083.

45. Hasin N, Cusack SA, Ali SS, Fitzpatrick DA, Jones GW. Global transcript and phenotypic analysis of yeast cells expressing Ssa1, Ssa2, Ssa3 or Ssa4 as sole source of cytosolic Hsp70-Ssa chaperone activity. BMC Genomics. 2014; 15:194. Epub 2014/03/19. https://doi.org/10.1186/1471-2164-15-194 PMID: 24628813; PubMed Central PMCID: PMC4022180.

46. Sharma D, Masison DC. Single methyl group determines prion propagation and protein degradation activities of yeast heat shock protein (Hsp)-70 chaperones Ssa1p and Ssa2p. Proc Natl Acad Sci U S A. 2011; 108(33):13665–70. Epub 2011/08/03. https://doi.org/10.1073/pnas.1107421108 PMID: 21808014; PubMed Central PMCID: PMC3158190.

47. Knighton LE, Nitika, Wolfgeher D, Reitzel AM, Truman AW. Dataset of Nematostella vectensis Hsp70 isoform interactomes upon heat shock. Data Brief. 2019; 27:104580. Epub 2019/11/02. https://doi.org/10.1016/j.dib.2019.104580 PMID: 31673583; PubMed Central PMCID: PMC6817661.

48. Knighton LE, Nitika, Waller SJ, Strom O, Wolfgeher D, Reitzel AM, et al. Dynamic remodeling of the interactomes of Nematostella vectensis Hsp70 isoforms under heat shock. Journal of proteomics. 2019; 206:103416. Epub 2019/06/25. https://doi.org/10.1016/j.jprot.2019.103416 PMID: 31233900; PubMed Central PMCID: PMC7304457.

49. Truman AW, Kristjansdottir K, Wolfgeher D, Ricco N, Mayampurath A, Volchenboum SL, et al. The quantitative changes in the yeast Hsp70 and Hsp90 interactomes upon DNA damage. Data Brief. 2015; 2:12–5. Epub 2015/07/29. https://doi.org/10.1016/j.dib.2014.10.006 PMID: 26217697; PubMed Central PMCID: PMC4459869.

50. Truman AW, Kristjansdottir K, Wolfgeher D, Hasin N, Polier S, Zhang H, et al. CDK-dependent Hsp70 Phosphorylation controls G1 cyclin abundance and cell-cycle progression. Cell. 2012; 151(6):1308–18. Epub 2012/12/12. https://doi.org/10.1016/j.cell.2012.10.051 PMID: 23217712; PubMed Central PMCID: PMC3778871.

51. Nitika, Zheng B, Ruan L, Kline JT, Sikora J, Torres MT, et al. A novel multifunctional role for Hsp70 in binding post-translational modifications on client proteins. bioRxiv. 2021:2021.08.25.457671. https://doi.org/10.1101/2021.08.25.457671

52. Roberts BT, Moriyama H, Wickner RB. [URE3] prion propagation is abolished by a mutation of the primary cytosolic Hsp70 of budding yeast. Yeast. 2004; 21(2):107–17. Epub 2004/02/03. https://doi.org/10.1002/yea.1062 PMID: 14755636.

53. Flower TR, Chesnokova LS, Froelich CA, Dixon C, Witt SN. Heat shock prevents alpha-synuclein-induced apoptosis in a yeast model of Parkinson's disease. J Mol Biol. 2005; 351(5):1081–100. https://doi.org/10.1016/j.jmb.2005.06.060 PMID: 16051265.

54. Gilbert CS, van den Bosch M, Green CM, Vialard JE, Grenon M, Erdjument-Bromage H, et al. The budding yeast Rad9 checkpoint complex: chaperone proteins are required for its function. EMBO Rep. 2003; 4(10):953–8. Epub 2003/09/16. https://doi.org/10.1038/sj.embor.embor935 PMID: 12973299; PubMed Central PMCID: PMC1326393.

55. Wyszkowski H, Janta A, Sztangierska W, Obuchowski I, Chamera T, Klosowska A, et al. Class-specific interactions between Sis1 J-domain protein and Hsp70 chaperone potentiate disaggregation of misfolded proteins. Proc Natl Acad Sci U S A. 2021; 118(49). Epub 2021/12/08. https://doi.org/10.1073/pnas.2108163118 PMID: 34873058; PubMed Central PMCID: PMC8670446.

56. Li J, Wu Y, Qian X, Sha B. Crystal structure of yeast Sis1 peptide-binding fragment and Hsp70 Ssa1 C-terminal complex. Biochem J. 2006; 398(3):353–60. Epub 2006/06/02. https://doi.org/10.1042/BJ20060618 PMID: 16737444; PubMed Central PMCID: PMC1559466.

57. Yu HY, Ziegelhoffer T, Craig EA. Functionality of Class A and Class B J-protein co-chaperones with Hsp70. FEBS Lett. 2015; 589(19 Pt B):2825–30. Epub 2015/08/08. https://doi.org/10.1016/j.febslet.2015.07.040 PMID: 26247431; PubMed Central PMCID: PMC4570866.

58. Johnson OT, Nadel CM, Carroll EC, Arhar T, Gestwicki JE. Two distinct classes of co-chaperones compete for the EEVD motif in heat shock protein 70 (Hsp70) to tune its activity. bioRxiv. 2021:2021.10.18.464838. https://doi.org/10.1101/2021.10.18.464838

59. Jones G, Song Y, Chung S, Masison DC. Propagation of Saccharomyces cerevisiae [PSI+] prion is impaired by factors that regulate Hsp70 substrate binding. Mol Cell Biol. 2004; 24(9):3928–37. Epub 2004/04/15. https://doi.org/10.1128/MCB.24.9.3928-3937.2004 PMID: 15082786; PubMed Central PMCID: PMC387751.

60. Gong W, Hu W, Xu L, Wu H, Wu S, Zhang H, et al. The C-terminal GGAP motif of Hsp70 mediates substrate recognition and stress response in yeast. J Biol Chem. 2018; 293(46):17663–75. Epub 2018/09/20. https://doi.org/10.1074/jbc.RA118.002691 PMID: 30228181; PubMed Central PMCID: PMC6240856.

61. Tao J, Berthet A, Citron YR, Tsiolaki PL, Stanley R, Gestwicki JE, et al. Hsp70 chaperone blocks alpha-synuclein oligomer formation via a novel engagement mechanism. J Biol Chem. 2021; 296:100613. Epub 2021/04/03. https://doi.org/10.1016/j.jbc.2021.100613 PMID: 33798554; PubMed Central PMCID: PMC8102405.

62. Truman AW, Bourboulia D, Mollapour M. Decrypting the chaperone code. J Biol Chem. 2021; 296:100293. Epub 2021/04/11. https://doi.org/10.1016/j.jbc.2021.100293 PMID: 33837727; PubMed Central PMCID: PMC7949055.

63. Nitika Porter CM, Truman AW Truttmann MC. Post-translational modifications of Hsp70 family proteins: Expanding the chaperone code. J Biol Chem. 2020; 295(31):10689–708. Epub 2020/06/11. https://doi.org/10.1074/jbc.REV120.011666 PMID: 32518165; PubMed Central PMCID: PMC7397107.

64. Backe SJ, Sager RA, Woodford MR, Makedon AM, Mollapour M. Post-translational modifications of Hsp90 and translating the chaperone code. J Biol Chem. 2020; 295(32):11099–117. Epub 2020/06/13. https://doi.org/10.1074/jbc.REV120.011833 PMID: 32527727; PubMed Central PMCID: PMC7415980.

65. Nitika Blackman JS, Knighton LE Takakuwa JE, Calderwood SK Truman AW. Chemogenomic screening identifies the Hsp70 co-chaperone DNAJA1 as a hub for anticancer drug resistance. Sci Rep. 2020; 10(1):13831. Epub 2020/08/17. https://doi.org/10.1038/s41598-020-70764-x PMID: 32796891; PubMed Central PMCID: PMC7429498.

66. Knighton LE, Nitika, Wani TH, Truman AW. Chemogenomic and bioinformatic profiling of ERdj paralogs underpins their unique roles in cancer. Cell Stress Chaperones. 2022. Epub 2022/02/08. https://doi.org/10.1007/s12192-022-01256-2 PMID: 35129801.

67. Sharma D, Masison DC. Functionally redundant isoforms of a yeast Hsp70 chaperone subfamily have different antiprion effects. Genetics. 2008; 179(3):1301–11. Epub 2008/06/20. https://doi.org/10.1534/genetics.108.089458 PMID: 18562668; PubMed Central PMCID: PMC2475734.

68. Jaiswal H, Conz C, Otto H, Wolfle T, Fitzke E, Mayer MP, et al. The chaperone network connected to human ribosome-associated complex. Mol Cell Biol. 2011; 31(6):1160–73. Epub 2011/01/20. https://doi.org/10.1128/MCB.00986-10 PMID: 21245388; PubMed Central PMCID: PMC3067906.

69. Tkach JM, Yimit A, Lee AY, Riffle M, Costanzo M, Jaschob D, et al. Dissecting DNA damage response pathways by analysing protein localization and abundance changes during DNA replication stress. Nat Cell Biol. 2012; 14(9):966–76. Epub 2012/07/31. https://doi.org/10.1038/ncb2549 PMID: 22842922; PubMed Central PMCID: PMC3434236.

70. Truman AW, Millson SH, Nuttall JM, Mollapour M, Prodromou C, Piper PW. In the yeast heat shock response, Hsf1-directed induction of Hsp90 facilitates the activation of the Slt2 (Mpk1) mitogen-activated protein kinase required for cell integrity. Eukaryot Cell. 2007; 6(4):744–52. Epub 2007/02/13. https://doi.org/10.1128/EC.00009-07 PMID: 17293484; PubMed Central PMCID: PMC1865661.

71. Zhang Y, Li H, Zhang C, An X, Liu L, Stubbe J, et al. Conserved electron donor complex Dre2-Tah18 is required for ribonucleotide reductase metallocofactor assembly and DNA synthesis. Proc Natl Acad Sci U S A. 2014; 111(17):E1695–704. Epub 2014/04/16. https://doi.org/10.1073/pnas.1405204111 PMID: 24733891; PubMed Central PMCID: PMC4035922.